Journal of Energy Storage 52 (2022) 105056

Contents lists available at ScienceDirect

Journal of Energy Storage

journal homepage: www.elsevier.com/locate/est

Research Papers

Exploring potential storage-based flexibility gains of electric vehicles in smart distribution grids

Afshin Pirouzi [a], Jamshid Aghaei [b,*], Sasan Pirouzi [a], Vahid Vahidinasab [c], Ahmad Rezaee Jordehi [d]

[a] Power System Group, Semirom Branch, Islamic Azad University, Semirom, Iran
[b] School of Energy Systems, Lappeenranta-Lahti University of Technology (LUT), Lappeenranta, Finland
[c] Department Engineering, School of Science and Technology, Nottingham Trent University, Nottingham NG11 8NS, UK
[d] Department of Electrical Engineering, Rasht Branch, Islamic Azad University, Rasht, Iran

ARTICLE INFO

Keywords:
Electric vehicle parking lot
Linear flexible power management
Renewable energy sources
Smart distribution network
Stochastic multiobjective formulation
Uncertainty

ABSTRACT

Flexibility is one of the most important solutions for facilitating the variability of renewable energy sources (RESs) in a distribution network. It is predicted that electric vehicles (EVs) can play an effective role in improving it in the distribution networks. So, this paper presents multiobjective scheduling of batteries of EVs in parking lots (EVPLs) to improve the storage-based flexibility of smart distribution networks (SDNs). The proposed formulation minimizes the energy cost and the voltage deviation function and maximizes the system flexibility (SF) as multiobjective functions that will be optimized subject to the AC load flow, RES and EV constraints, and the allowable limits of the flexibility and operation indices. The resulting model is in the form of a nonlinear programming (NLP) model. Therefore, an equivalent linear programming (LP) formulation is obtained for the original problem to achieve the global optimum result. The stochastic programming approach is used to model uncertainties of the load, active power generation of RESs, price of energy, and EV parameters. The flexible power management is formulated as one of the objective functions of the proposed multiobjective framework, which is solved by using the ε-constraint method, reaching the best possible compromise solution by a fuzzy decision-maker. The proposed framework is tested by using a 33-bus radial test distribution network in the GAMS software environment to evaluate the EVs capability in improving the flexibility indices. Based on the numerical results, it is observed that the proposed scheme with optimal energy management of EVs is able to obtain a high flexibility for SDN. It can also reduce energy losses in terms of network operation and provide a rather smooth voltage profile.

1. Introduction

1.1. Motivation

The past two decades have witnessed the proliferation of renewable energy sources (RESs), such as wind turbines (WT) and solar photovoltaics (PVs), aiming to reduce the environmental pollution in green smart distribution networks (SDNs). However, these resources have raised some concerns regarding the increased uncertainty of network operation, and as a result, they have reduced the system flexibility (SF). Flexibility is introduced as "*the modification of generation injection and/or consumption patterns in reaction to an external price or activation signal in order to provide a service within the electrical system*" [1]. There are different flexible resources such as demand response programs (DRPs) [2], fuel cells, nonrenewable energy sources (NRESs) such as gas-fuelled microturbines and diesel generators [3], and electrical energy storage systems (ESSs) [4]. Furthermore, it should be noted that electric vehicles (EVs) are mobile storage systems, which can be charged/discharged by/into the distribution networks. Therefore, the EVs in parking lot (EVPL) parking lot/aggregator can be considered a flexible resource with an acceptable response time, because an EV includes a battery that could provide a high flexibility. This is due to the inherent fast dynamics combined with the fast control possibility based on power electronic converters [5].

* Corresponding author.
E-mail addresses: jamshid.aghaei@lut.fi (J. Aghaei), vahid.vahidinasab@ntu.ac.uk (V. Vahidinasab).

https://doi.org/10.1016/j.est.2022.105056
Received 17 January 2022; Received in revised form 30 May 2022; Accepted 3 June 2022
Available online 10 June 2022
2352-152X/© 2022 The Authors. Published by Elsevier Ltd. This is an open access article under the CC BY license (http://creativecommons.org/licenses/by/4.0/).

Nomenclature

k, Ω_k Index and set (I/S) of linearized pieces of the circular constraint, respectively
l, Ω_l I/S of linearized pieces of the voltage magnitude, respectively
n, j, Ω_b I/S of bus, respectively
n_c, n_v Total number of the linearized pieces of the circular constraint and voltage, respectively
ref Index of the slack (reference) bus
t, Ω_t I/S of time, respectively
w, Ω_s I/S of scenario, respectively

Variables
B, C Active/reactive power of the batteries/chargers, respectively [p.u.]
E Total stored energy of the EV batteries in the EVPL [p.u.]
f_1, f_2, f_3 Expected energy cost [\$], voltage deviation function [p.u.], and symmetry of the system flexibility
F^p, F^q Active/reactive flows of lines, respectively [p.u.]
L^p, L^q Active/reactive losses of chargers in the EVPLs [p.u.]
P^E, Q^E Total active/reactive power of the EVs from the grid's point of view [p.u.]
P^{E+}, P^{E-} Total charging/discharging of the EVs from the grid's point of view [p.u.]
P^G, Q^G Active/reactive power of the distribution substation [p.u.]
SF System flexibility [without unit]
U^f, D^f Total upward/downward storage-based flexibility of EVs in an EVPL, respectively [p.u.]
V, ΔV, δ Amount, deviation, and angle of voltage, respectively [radian]

Constant values
A Incidence matrix of lines (e.g., $A_{x,y}$ is equal to 1 provided that there is a line between buses x and y and otherwise is 0)
a_p, a_q Loss function coefficients of a charger
b_p, b_q Coefficients of the reactive power loss of a charger
CR, DR Rate of charging/discharging of EV batteries, respectively [p.u.]
CC^{max} Maximum capacity of chargers in an EVPL [p.u.]
D^p, D^q Active and reactive loads, respectively [p.u.]
E^{ini}, E^{final} Level of the initial/final energy of EVs in EVPL [p.u.]
F^{max}, G^{max} Maximum line/substation capacity, respectively [p.u.]
g, b Conductance and susceptance of each branch, respectively [p.u.]
k_Q Ratio of active power price with respect to reactive power price
L, AER Distance and all electric ranges that an EV can drive, respectively [mi]
M Line slope for a linear piece
P^R Active power output of an RES [p.u.]
SOC, BC State of charge and capacity of EV batteries, respectively
TPF Tangent value in the minimum power factor point
V^{max}, V^{min} Maximum/minimum amount of voltage at each bus, respectively [p.u.]
V_{ref} Voltage of the slack bus [p.u.]
ΔV^{max} Maximum amount of voltage deviation [p.u.]
ρ Price of energy [\$/MWh]
π Probability of each scenario
$\Delta\alpha$ Angle deviation [radian]

1.2. Literature review

There are numerous studies in the field of optimal scheduling of EVs in distribution networks. For instance, in [6], the authors propose optimal charging scheduling of EVs in distribution networks based on the day-ahead market price to obtain a low charging cost to all EVs. Furthermore, charging management of EVs in charging stations based on centralized and decentralized methods is presented in [7], where a linear optimization model is used to obtain EV charging scheduling. In [8], day-ahead electricity procurement and real-time EV charging management of an aggregator are formulated by a two-stage charging framework for EVs in order to reduce the operating costs. In [9], the EV charging scheduling is investigated in distribution networks where an optimal AC power flow is used based on the model predictive control to obtain a low energy cost and optimal hourly EV demand power or energy. Moreover, multistage optimization is used in [10] to manage the charging demand of EVs in active distribution networks considering a coordination framework for all EVs. The authors of [11] present a bilevel scheduling scheme for an isolated microgrid including RESs by incorporating demand response of EVs. In [12], the Lyapunov optimization is used to determine the EV scheduling based on a low energy cost while considering the uncertainty of RESs. In addition, a game theoretic decentralized EV charging strategy is presented in [13] to achieve minimum payments for customers, maximum grid efficiency, and maximum potential capacity of EVs in the regulation services. Moreover, the EV charging management is discussed in [14] to maximize cost efficiency and user convenience. The method of [14] is also repeated in [15] according to the user's charging selection strategy based on economic indices. It is used in [16] by considering EVs and network objectives while defining an optimal power flow problem. Finally, in [17], a real-time EV charging scheduling is obtained in the distribution network in the presence of PVs and ESSs.

Ref. [18] proposes several strategies to optimally allocate EV charging stations and discusses their influence on distribution networks. Proper size of hybrid RESs is determined and optimized in [19]. The same reference also investigates the potential of sharing power with EVs. Multi-objective particle swarm optimization and multi-objective crow search as two popular algorithms are adopted to address the problem. A two-stage framework has been discussed in [20]. The first stage deals with analyzing some parameters including battery status, charge/discharge modes, together with transportation parameters like distance traversed within a given day, times of EVs arrival and departure to parking lots, and the amount of EV sales, and the profitability of the EV charging/discharging program for EV users have been calculated. The other stage deals with the influence of parking lots and the imbalance indices have been calculated. A novel decentralized bi-level stochastic optimization approach based on the progressive hedging algorithm has been proposed in [21] for multi-agent systems in multi-energy microgrids so that flexibility is improved. A probabilistic nonlinear model has been suggested in [22] based on power flow study to maximize the flexibility in which EVs limitations have been considered. Some essential items discussed include improving voltage profile and congestion, and providing robust thermal comfort during reserve call, and exploiting multi-energy storages. The strategic scheduling of a multi-energy system (MES) in the day-ahead wholesale market has been presented in [23]. The model formulates a bi-level optimization problem. The upper-level minimizes the cost of the MES, and the lower-level deals with the wholesale market operator so that public satisfaction has been maximized. The authors in [24] put forward a framework to obtain proper locational marginal prices of reserves, which include up−/down-going reserves at both generation- and demand-sides. A hybrid island system consisting of a wind turbine, PV, diesel generator, and stationary (battery) and mobile (EVs) ESS has been presented in [25]. The method deploys a multi-objective optimization to find minimum costs associated with investment, maintenance and repair, and operation of power sources and ESSs besides reducing pollution level. Intelligent parking lots (IPLs) in an uncertain environment are managed in [26] and optimal bidding curves are achieved concerning the power market. The paper also attempts to find the optimal bidding curves while taking into account the uncertainty associated with power price and optimal operation of IPLs. Empirical mode decomposition, feature selection, and hybrid forecast engine have been used in [27] to propose a novel prediction model. The model incorporates non-stationarity and non-convex nature of the wind power signal. A combined energy system composed of a parabolic dish solar collector, a Stirling engine, and thermoelectric device have been examined in [28]. Short-term power prediction of wind and PV power to evaluate the output power of production units has been discussed in [29]. The model uses lead acid batteries in a hybrid wind turbine/PV system. To find maximum profit of a compressed air energy system, the authors in [30] have presented a novel mathematical formulation which plays the role of a hybrid robust-stochastic approach. The study also deals with uncertain price of the market by using several scenarios using the stochastic method. Besides, maximum uncertain size of cavern has been modeled with the help of a robust optimization formulation. Table 1 provides a summary of the background research.

1.3. Contributions

Within the literature in the area, there are main research gaps as follows:

- There are numerous studies that consider the energy management of EVPLs to obtain a low energy or operating cost; in these studies, nonlinear programming (NLP) optimization is usually applied to obtain optimal EV charging/discharging scheduling in the distribution network. Nevertheless, EVs can be entered into ancillary services, such as voltage regulation and reactive power market, if they use bidirectional chargers [31]. Moreover, it is noted that EVs can participate in the SF management, which is an important method in SDNs in the presence of RESs; however, this matter has received little attention in studies on EV's energy management.
- There are various economic and technical indices in SDN, where an improvement in one indicator does not necessarily improve the status of another. This requires simultaneous modeling of different SDN indices, which according to Table 1, this has not been discussed in any research.
- Most research has generally suggested that the presence of RES in the network will reduce network flexibility, then suggested the use of ESS and DRP to improve flexibility. Nonetheless, they did not provide a numerical indicator of flexibility. However, to estimate the status of an indicator, it is necessary to know its value.

Therefore, this paper for fill the research gaps, as shown in Fig. 1, presents a multiobjective optimization model to achieve the optimal power management of EVs in improving the SF, voltage regulation, reactive power services, and energy management of distribution networks. Accordingly, the proposed flexible power management minimizes the energy cost and voltage deviation and maximizes the SF in a multiobjective optimization framework subject to the optimal AC power

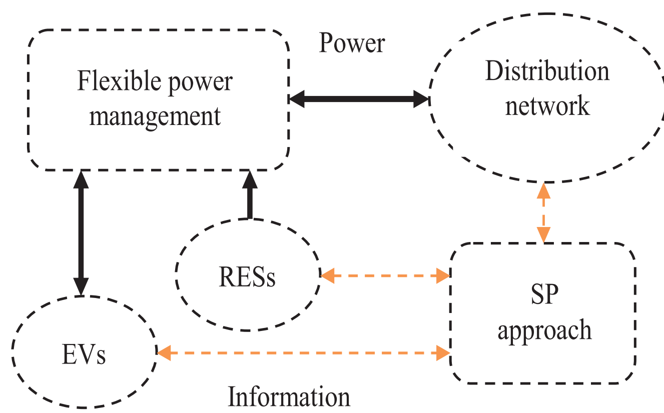

Fig. 1. Conceptual framework of stochastic flexible SDN management.

Table 1
Taxonomy of recent research works.

Ref.	Indices			formulation of flexibility	EVPL as flexibility source	Problem model
	Economic	Operation	Flexibility			
[6]	Yes	Yes	No	No	No	Non-linear
[7]	No	Yes	No	No	No	Non-linear
[8]	No	Yes	No	No	No	Non-linear
[9]	Yes	Yes	No	No	No	Non-linear
[10]	No	Yes	No	No	No	Non-linear
[11]	No	Yes	No	No	No	Linear
[12]	Yes	Yes	No	No	No	Non-linear
[13]	No	Yes	No	No	No	Non-linear
[14]	Yes	Yes	No	No	No	Non-linear
[15]	Yes	Yes	No	No	No	Non-linear
[16]	No	Yes	No	No	No	Non-linear
[17]	No	Yes	No	No	No	Non-linear
[18]	Yes	Yes	No	No	No	Non-linear
[19]	Yes	Yes	No	No	No	Non-linear
[20]	No	Yes	No	No	No	Non-linear
[21]	No	Yes	No	No	No	Non-linear
[22]	No	Yes	Yes	No	No	Non-linear
[23]	Yes	Yes	No	No	No	Non-linear
[24]	No	Yes	No	No	No	Non-linear
[25]	Yes	Yes	No	No	No	Linear
[26]	No	Yes	No	No	No	Non-linear
[27]	No	Yes	No	No	No	Non-linear
[28]	No	Yes	No	No	No	Non-linear
[29]	No	Yes	No	No	No	Linear
[30]	Yes	Yes	No	No	No	Non-linear
Proposed scheme	Yes	Yes	Yes	Yes	Yes	Linear

flow equations in the presence of EVs and RESs. The proposed NLP model is converted into linear programming (LP) by using the first-order term of a Taylor series to linearize the AC load flow equations and replacing a polygon for circular constraints, such as the capacity limit of the distribution lines. In the next step, the hybrid ε-constraint and fuzzy decision-making method is used to obtain single-objective formulation. The proposed framework also takes into account the uncertainty of load, price of energy, RESs power, and energy demand and charger capacity of EVs. Therefore, stochastic programming (SP) is used to model these parameters according to the Monte Carlo simulation (MCS)-based scenario generation approach and the fast backward/forward scenario reduction method. Considering the aforementioned literature review, the novel aspects of this work can be stated as follows:

– Modeling of the multiobjective flexible management of SDNs for achieving a flexible network with improved technical indices;
– Obtaining the optimal potential of EVs to increase storage-based flexibility, regulate the voltage profile, provide reactive power services, and facilitate energy management.
– Modeling the economic, operation and flexibility indices, simultaneously.

1.4. Objectives and hypothesis

Objectives

– Considering EVs as flexibility source,
– Investigate the EVs capability on the economic and operation sections of SDN,
– Flexibility modeling,
– Modeling the economic, operation and flexibility indices, simultaneously,
– Investigate the EVs capability on the active and reactive power management.
– Hypothesis
– EVs can be considered as flexibility source,
– EVs can be modified the operation indices of SDN, i.e. energy loss, voltage profile and energy cost.

1.5. Paper organization

The rest of the paper is organized as follows. In Section 2, linear and nonlinear modeling for multi-objective and single-objective problems is presented. Then, the modeling of uncertainties is presented in Section 3. Finally, the numerical results and conclusions are presented in Sections 4 and 5, respectively.

2. Optimal flexible scheduling of electric vehicles

2.1. Original nonlinear formulation

The original nonlinear formulation of the optimal flexible scheduling of EVs is presented in this subsection. As it can be seen, the objective is to minimize the total energy cost (EC) and the voltage deviation function (VDF) and also to maximize the SF. The model is solved subject to the AC load flow constraints in the presence of EVs and RESs and operational and flexibility constraints. The problem is formulated in Eqs. (1)–(23) as follows:

$$min_{P^E,Q^E}\begin{cases} f_1=\sum_{w\in\Omega_s}\pi_w\sum_{t\in\Omega_t}\rho_{t,w}\left(P^G_{ref,t,w}-\overbrace{\sum_{n\in\Omega_b}\left(P^{E-}_{n,t,w}+k_Q\left|Q^E_{n,t,w}\right|\right)}^{EVsrevenue}\right) \\ f_2=\sum_{w\in\Omega_s}\pi_w\sum_{n\in\Omega_b}\sum_{t\in\Omega_t}\left(V_{n,t,w}-V_{ref}\right)^2 \\ f_3=-SF\end{cases}\forall\sum_{w\in\Omega_s}\pi_w=1 \tag{1}$$

Subject to:

$$P^G_{n,t,w}-P^E_{n,t,w}-\sum_{j\in\Omega_b}A_{n,j}F^p_{n,j,t,w}=D^p_{n,t,w}-P^R_{n,t,w}\quad\forall\ n,\ \ t,w \tag{2}$$

$$Q^G_{n,t,w}-Q^E_{n,t,w}-\sum_{j\in\Omega_b}A_{n,j}F^q_{n,j,t,w}=D^q_{n,t,w}\quad\forall\ n,\ \ t,w \tag{3}$$

$$F^p_{n,j,t,w}=g_{n,j}\left(V_{n,t,w}\right)^2-V_{n,t,w}V_{j,t,w}\left\{g_{n,j}cos\left(\delta_{n,t,w}-\delta_{j,t,w}\right)+b_{n,j}sin\left(\delta_{n,t,w}-\delta_{j,t,w}\right)\right\}\quad\forall n,j,t,w \tag{4}$$

$$F^q_{n,j,t,w}=-b_{n,j}\left(V_{n,t,w}\right)^2+V_{n,t,w}V_{j,t,w}\left\{b_{n,j}cos\left(\delta_{n,t,w}-\delta_{j,t,w}\right)-g_{n,j}sin\left(\delta_{n,t,w}-\delta_{j,t,w}\right)\right\}\quad\forall n,j,t,w \tag{5}$$

$$V_{n,t,w}=V_{ref}\quad\forall\ n=\text{Slack bus},\ \ t,w \tag{6}$$

$$\delta_{n,t,w}=0\quad\forall\ n=\text{Slack bus},\ \ t,w \tag{7}$$

$$V^{\min}\le V_{n,t,w}\le V^{\max}\quad\forall\ n,\ \ t,w \tag{8}$$

$$\sqrt{\left(F^p_{n,j,t,w}\right)^2+\left(F^q_{n,j,t,w}\right)^2}\le F^{\max}_{n,j}\quad\forall\ n,j,\ \ t,w \tag{9}$$

$$\sqrt{\left(P^G_{n,t,w}\right)^2+\left(Q^G_{n,t,w}\right)^2}\le G^{\max}_n\quad\forall\ n,t,w \tag{10}$$

$$-TPF\times P^G_{n,t,w}\le Q^G_{n,t,w}\le TPF\times P^G_{n,t,w}\quad\forall\ n=\text{Slack bus},\ \ t,w \tag{11}$$

$$P^E_{n,t,w}=B_{n,t,w}+L^p_{n,t,w}\quad\forall\ n,\ \ t,w \tag{12}$$

$$Q^E_{n,t,w}=C_{n,t,w}+L^q_{n,t,w}\quad\forall\ n,\ \ t,w \tag{13}$$

$$P^E_{n,t,w}=P^{E+}_{n,t,w}-P^{E-}_{n,t,w}\quad\forall\ n,\ \ t,w\ \&P^{E+},P^{E-}\ge 0 \tag{14}$$

$$L^p_{n,t,w}=a_p\left(P^{E+}_{n,t,w}+P^{E-}_{n,t,w}\right)+a_q\left|Q^E_{n,t,w}\right|\quad\forall\ n,t,w \tag{15}$$

$$L^q_{n,t,w}=b_p\left(P^{E+}_{n,t,w}+P^{E-}_{n,t,w}\right)+b_q\left|Q^E_{n,t,w}\right|\quad\forall\ n,t,w \tag{16}$$

$$-DR_{n,t,w}\le B_{n,t,w}\le CR_{n,t,w}\quad\forall\ n,t,w \tag{17}$$

$$\sqrt{\left(P^E_{n,t,w}\right)^2+\left(Q^E_{n,t,w}\right)^2}\le CC^{\max}_{n,t,w}\quad\forall\ n,t,w \tag{18}$$

$$E_{n,t,w}=E_{n,t-1,w}+B_{n,t,w}\quad\forall n,t,w\ \&E\ge 0 \tag{19}$$

$$E_{n,t,w}=E^{ini}_{n,t,w}\quad\forall n,t=\text{Arrival time},w \tag{20}$$

$$E_{n,t,w}=E^{final}_{n,t,w}\quad\forall n,t=\text{Departure time},w \tag{21}$$

$$U^f_{n,t,w}-D^f_{n,t,w}=P^E_{n,t,w}-P^E_{n,t,1}\quad\forall n,t,w\ne 1\ \&U^f,D^f\ge 0 \tag{22}$$

$$SF=\sum_{n,t,w}\pi_w.\frac{U^f_{n,t,w}+D^f_{n,t,w}}{2\times CC^{\max}_{n,t,w}} \tag{23}$$

Eq. (1) presents the multiobjective functions that include minimization of the cost of buying energy from the main grid (upstream network) (f_1) [32], minimization of the voltage deviation function (f_2) [33], and maximization of the SF (f_3) [32]. In f_1, the energy cost is equal to the difference between the summation of demand, power loss, and EV charging cost and EV revenue resulting from the injection of active power and injection/absorption of reactive power into/from the network. Constraints (2)–(7) express the AC load flow equations considering the RESs and EVPLs. Eqs. (2) and (3) are the active and reactive power balance between different sources (distribution substation and RESs) and active loads (i.e., EVs) and passive ones. Further, Eqs. (4) and (5) are the active and reactive flows of distribution branches, and in Eqs. (6) and (7), the voltage level and angle of the slack bus are set. Here, it is assumed that the distribution substation connects to the slack bus, and therefore, the amounts of P^G and Q^G at all buses, except the slack bus, are considered zero. Moreover, the system operation limits are presented in Eqs. (8)–(11), where they are the limits of voltage magnitude, line apparent power flow (line capacity), capacity and power factor, respectively, of the distribution station. In Eq. (11), *TPF* is the tangent value in the minimum power factor point (here, it is 0.90).

The constraints of EVPLs are presented in Eqs. (12)–(21). Eq. (12) models the active power balance of the network and the total of batteries in the EVPLs, Eq. (13) is the reactive power balance of the network and the total of chargers in the EVPLs, Eq. (14) is the active power equation of EVs based on their charging and discharging power, Eqs. (15) and (16) are active and reactive power losses for all EVs chargers in the EVPL, Eq. (17) is the charge/discharge limit for all EV batteries in the EVPL, Eq. (18) is the capability curve of the EVPLs, Eq. (19) is the amount of stored energy in all EV batteries, and Eq. (20) and (21) are the energy of EV batteries at arrival and departure time, respectively. Note that E^{ini} at time t is equal to $\sum_{e=1}^{NI_t} SOC_e BC_e$, in which the *SOC* and *BC* are the state of charge and capacity of the EV battery, and NI_t is the total number of EVs connected to the network in an EVPL at time t. Further, *SOC* shows the percentage of energy remaining in the battery when the EV arrives the EVPL after daily journeys. Therefore, it is subject to the distance that the EV drives (L) as well as all electrical ranges (*AER*) based on the equation $SOC = (1 - L/AER)$ [34]. *AER* demonstrates the total distance that an EV can drive based on the capacity of its battery. Finally, it is assumed that each EV charges its battery to the full charge, and hence, E^{final} is equal to $\sum_{e=1}^{NF_t} BC_e$, where NF_t is the total number of EVs disconnected from an EVPL at time t.

In this work, a metric is proposed to quantify the technical level of storage-based flexibility in both the individual flexible resource (EVPLs) and the whole system [35]. The proposed metric helps in analyzing the technical ability of a system or resources to cope with the flexibility requirement resulting from the variability and uncertainty produced by RESs. The flexibility index for each resource comprises two parts, upward and downward flexibility [36]. There is upward flexibility for a flexible resource if its output power in scenario k is greater than its output power in the base case (scenario 1). But if the output power of a flexible resource in scenario k is less than its output power in the base case, there is downward flexibility for the flexible resource [36]. Therefore, the upward and downward flexibilities for the EVPLs can be obtained from Eq. (22). Moreover, the SF is calculated based on Eq. (23) [35]. Here, B and C are the decision variables of the aforementioned optimization model, and f_1 to f_3 are the output variables. In addition, it is pointed out that this paper investigates the capability of EVs to provide storage-based flexibility in an SDN, and other potential flexible resources, such as DRPs, ESSs, and NRES, are neglected. Furthermore, it is assumed that the distribution network is balanced, and as a result, all the loads and EVs are equally distributed among the different three phases of the electricity network.

2.2. Linear approximated model

Owing to the nonlinear equations of f_1 and f_2 in Eqs. (1), and (4), (5), (9), (10), (15), (16), and (18), and nonconvex Eqs. (4) and (5), the base model in Eqs. (1)–(23) is modeled as a nonconvex NLP problem. Therefore, the solvers of this method are based on numerical techniques, and in the best situation, because of the nonconvex equations, they obtain the local optimal point [32,33]. It is noted, however, that this method can be converted into a linear approximation model by considering a suitable assumption for different variables and equations. For example, the distribution network is generally inductive, and hence, the reactive power control devices, such as EVs, operate in the capacitive mode ($Q^E \le 0$). Therefore, the term of $|Q^E|$ is converted into $-Q^E$ in Eqs. (1), (15), and (16). Furthermore, based on [19], the difference between the angles of the two ends of a line (i.e., δ_n - δ_j) is <0.105. Therefore, the terms of cos(δ_n - δ_j) and sin(δ_n - δ_j) are approximated as 1 and (δ_n - δ_j), respectively. Moreover, based on the conventional piecewise linearization technique, the voltage magnitude can be expressed as $V^{\min} + \sum_{l\in\varphi_l} \Delta V_l$ [19], where $\Delta V << 1$. Thus, the expressions of V^2 and $V_n V_j$ are formulated as $\left(V^{\min}\right)^2 + \sum_{l\in\varphi_l} m_l \Delta V_l$and $\left(V^{\min}\right)^2 + V^{\min}\sum_{l\in\varphi_l}\Delta V_{b,l} + V^{\min}\sum_{l\in\varphi_l}\Delta V_{j,l}$, respectively. Finally, the linear approximation equations for Eqs. (4), (5), (8), and f_2 are rewritten as follows:

$$F^p_{n,j,t,w} = g_{n,j}\left(\sum_{l\in\Omega_l}\left(m_l - V^{\min}\right)\Delta V_{n,t,w,l} - V^{\min}\Delta V_{j,t,w,l}\right) - \left(V^{\min}\right)^2 b_{n,j}\left(\delta_{n,t} - \delta_{j,t}\right) \quad \forall n,j,t,w \tag{24}$$

$$F^q_{n,j,t,w} = -b_{n,j}\left(\sum_{l\in\Omega_l}\left(m_l - V^{\min}\right)\Delta V_{n,t,w,l} - V^{\min}\Delta V_{j,t,w,l}\right) - \left(V^{\min}\right)^2 g_{n,j}\left(\delta_{n,t} - \delta_{j,t}\right) \quad \forall n,j,t,w \tag{25}$$

$$0 \le \Delta V_{n,t,w,l} \le \Delta V^{\max} \quad where\ \Delta V^{\max} = \frac{V^{\max} - V^{\min}}{n_v} \quad \forall\ n,\ \ t,w,l \in \Omega_l = \{1,2,\dots,n_v\} \tag{26}$$

$$f_2 = \sum_{w\in\Omega_s}\pi_w \sum_{n\in\Omega_b}\sum_{t\in\Omega_t}\left\{\left(V_{ref} - V^{\min}\right)^2 + \sum_{l\in\Omega_l}\left(m_l - 2V_{ref}\right)\Delta V_{n,t,w,l}\right\} \tag{27}$$

It is to be noted that Eqs. (9), (10), and (18) are circular inequalities, which can be approximated by a polygon. As it is shown in Fig. 2, each side of the polygon is a straight line, and thus, its equation can be obtained [32,33]. Accordingly, the constraints (9), (10), and (18) are linearized as follows:

$$F^p_{n,j,t,w} cos(k \times \Delta\alpha) + F^q_{n,j,t,w} sin(k \times \Delta\alpha) \le F^{\max}_{n,j} \ where\ \Delta\alpha = \frac{2\pi}{n_c}\ \forall\ n,j,\ \ t,w,k \in \Omega_k = \{1,2,\dots,n_c\} \tag{28}$$

Therefore, the equivalent LP model of the base problem can be reformulated as Eqs. (31)–(34), where it is suitable to obtain the global optimal point, and its solvers, such as the simplex method, can be calculated with the values of different variables at a lower time or a higher speed [32,33].

$$min_{P^E,Q^E}\begin{cases} f_1=\sum_{w\in\Omega_s}\pi_w\sum_{t\in\Omega_t}\rho_{t,w}\left(P^G_{ref,t,w}-\sum_{n\in\Omega_b}\left(P^{E-}_{n,t,w}-k_QQ^E_{n,t,w}\right)\right)\\ f_2=\sum_{w\in\Omega_s}\pi_w\sum_{n\in\Omega_b}\sum_{t\in\Omega_t}\left\{\left(V_{ref}-V^{\min}\right)^2+\sum_{l\in\Omega_l}\left(m_l-2V_{ref}\right)\Delta V_{n,t,w,l}\right\}\\ f_3=-SF\end{cases}\quad\forall\sum_{w\in\Omega_s}\pi_w=1,Q^E_{n,t,w}\le 0 \tag{31}$$

Subject to:

$$\text{Constraints }(2),(3),(6)\text{–}(7),(11)\text{–}(14),(17),(19)\text{–}(26),\text{ and }(28)\text{–}(30) \tag{32}$$

$$L^p_{n,t,w}=a_p\left(P^{E+}_{n,t,w}+P^{E-}_{n,t,w}\right)-a_qQ^E_{n,t,w}\quad\forall\ n,t,w \tag{33}$$

$$L^q_{n,t,w}=b_p\left(P^{E+}_{n,t,w}+P^{E-}_{n,t,w}\right)-b_qQ^E_{n,t,w}\quad\forall\ n,t,w \tag{34}$$

2.3. Single-objective LP model

In this paper, multiobjective optimization is used to achieve the Pareto optimal solutions of the problem and present them to the decision-maker to choose the final solution among the Pareto solutions. There are different techniques for Pareto optimization [37], of which this paper uses the ε-constraint to obtain a linear model for single-objective function formulation [37]. Based on this approach [37], one objective function is considered the main one, and all the other objective functions are defined as inequality constraints with a maximum value of ε. For the proposed problem, Eqs. (31)–(34), f_1 is minimized, but f_2 and f_3 are constrained to ε_2 and ε_3, respectively, according to the following formulation:

$$min_{P^E,Q^E}\ f_1 \tag{35}$$

Subject to:

$$\text{Constraints }(32)\text{–}(34) \tag{36}$$

$$f_2\le\varepsilon_2\quad\forall\varepsilon_2\in\left[f_2^{\min},f_2^{\max}\right] \tag{37}$$

$$f_3\le\varepsilon_3\quad\forall\varepsilon_3\in\left[f_3^{\min},f_3^{\max}\right] \tag{38}$$

It is noted that the terms of ε_2 and ε_3 are control parameters of the proposed method, where they change between the minimum and maximum values ($f^{\min}$ and $f^{\max}$) of different objective functions based on Eqs. (37) and (38). To calculate $f^{\min}$ and $f^{\max}$, problem (31)–(34) is solved for each objective function separately. Finally, to obtain the best compromise solution, this paper uses the fuzzy decision-making method [37] that calculates the linear fuzzy membership function ($\widehat{f}$) as follows:

$$\widehat{f}_i=\begin{cases}1 & f_i\le f_i^{\min}\\ \dfrac{f_i-f_i^{\max}}{f_i^{\min}-f_i^{\max}} & f_i^{\min}\le f_i\le f_i^{\max}\\ 0 & f_i^{\max}\le f_i\end{cases}\qquad i=1,2,3 \tag{39}$$

where $\widehat{f}$ varies between 0 and 1. In the next step, the fuzzy decision-maker calculates min{f_1, f_2, f_3} for different values of ε_2 and ε_3, and thus, this method will yield the best compromise solution by calculation

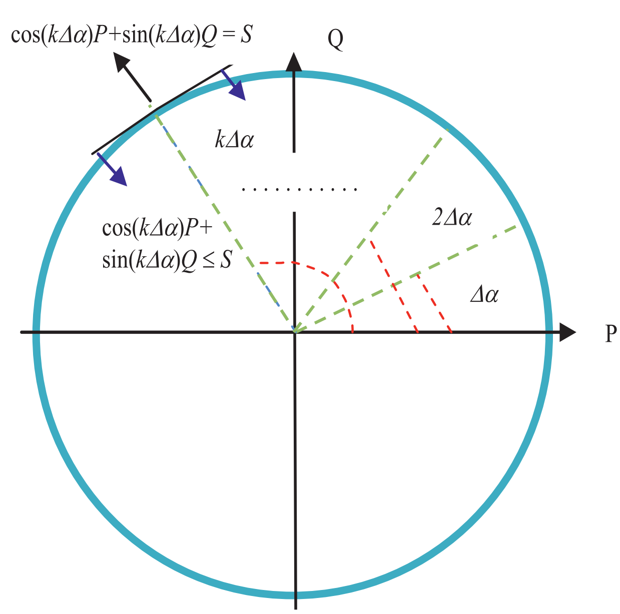

Fig. 2. Linearization method for circular inequality [32]

$$P^G_{n,t,w}cos(k\times\Delta\alpha)+Q^G_{n,t,w}sin(k\times\Delta\alpha)\le G_n^{\max}\quad\forall\ n,t,w,k \tag{29}$$

$$P^E_{n,t,w}cos(k\times\Delta\alpha)+Q^E_{n,t,w}sin(k\times\Delta\alpha)\le CC^{\max}_{n,t,w}\quad\forall\ n,t,w,k \tag{30}$$

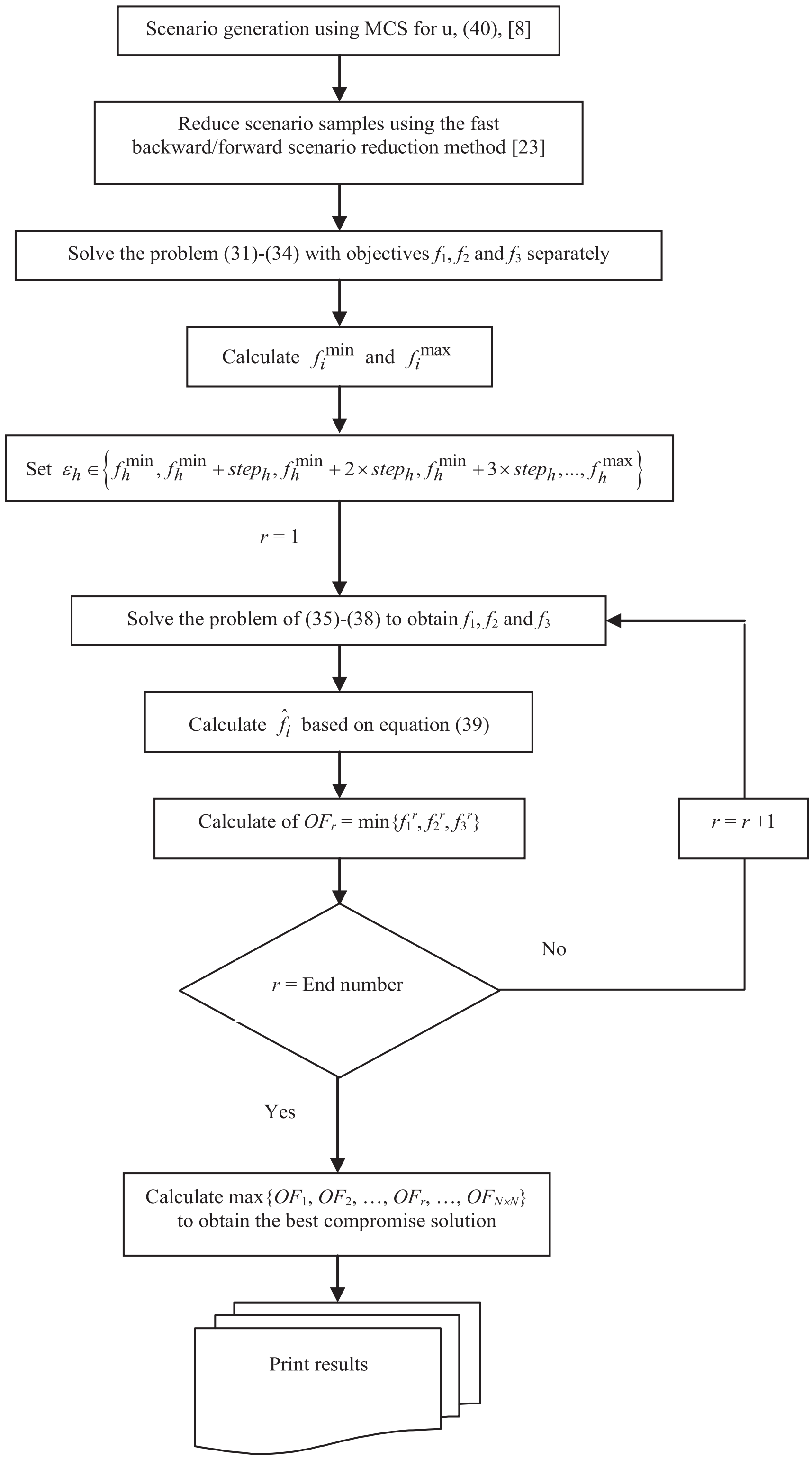

Fig. 3. Flowchart of the proposed solving approach.

of the maximum value of the previous step. Finally, Algorithm 1 presents the proposed approach to calculate the optimal compromise point in problem (35)–(38).

$$u = \left[D^p\ D^p\ P^R\ \rho\ CR\ DR\ CC^{\max}\ E^{ini}\ E^{final}\right] \tag{40}$$

In this paper, the MCS is applied for modeling these uncertain parameters by scenario generation. Each scenario of the MCS is generated considering the following points:

Algorithm 1 ε-constraint method based on Pareto optimization

1: Solve the problem (31)–(34) with the separate objectives of f_1, f_2, and f_3 to obtain the value of these objectives.
2: Calculate $f_i^{\min}$ and $f_i^{\max}$, where $i = 1, 2, 3$.
3: Set $\varepsilon_h \in \left\{f_h^{\min}, f_h^{\min}+step_h, f_h^{\min}+2\times step_h, f_h^{\min}+3\times step_h, \ldots, f_h^{\max}\right\}$, where $h = 2, 3$. The term *step* is equal to $(f^{max} - f^{min})/N$, and N is the total segments between f^{min} and f^{max} with the size of the *step*.
4: Solve the problem (35)–(38) to obtain f_1, f_2, and f_3.
5: Calculate $\hat{f}_i$ based on (39), where $i = 1, 2, 3$.
6: Calculate $OF_r = \min\{f_1^r, f_2^r, f_3^r\}$, where r = 1, 2, …, $N\times N$.
7: Calculate $\max\{OF_1, OF_2, \ldots, OF_r, \ldots, OF_{N\times N}\}$ to obtain the best compromise solution.

- The load and energy price forecast errors at each hour and bus are based on the normal (Gaussian) probability distribution function [36].
- EV parameter forecasts for each bus and hour are based on the Rayleigh probability distribution function [38].

After that, the fast backward/forward approach for scenario reduction is used to reduce the number of scenario samples and enhance the tractability of the proposed LP operational tool [39]. Finally, a flowchart of the solving approach based on Algorithm 1 and the proposed scenario generation/reduction method is illustrated in Fig. 3.

3. Uncertainty modeling

There are various uncertain parameters, such as active and reactive demands (D^p and D^q), output power of RESs (P^R), energy price (ρ), total charge/discharge rate of the EV batteries (CR/DR), charger capacity of all EVs in the EVPL (CC^{max}), and the initial and final energy of EVs (E^{ini} and E^{final}). Therefore, the uncertainty matrix is written as follows:

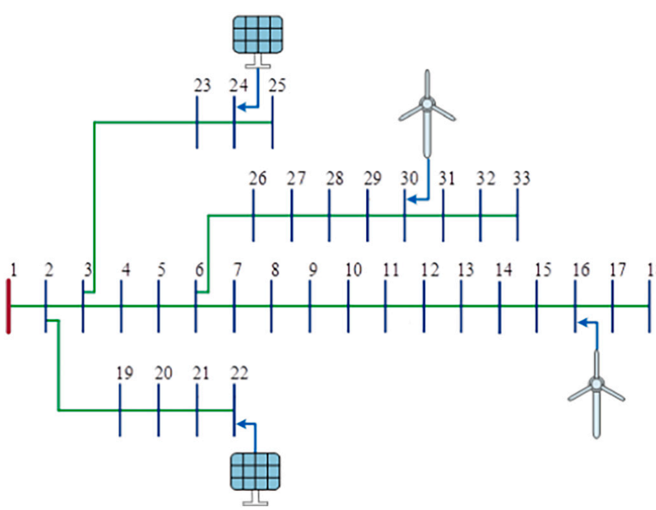

Fig. 4. 33-bus test distribution network [40].

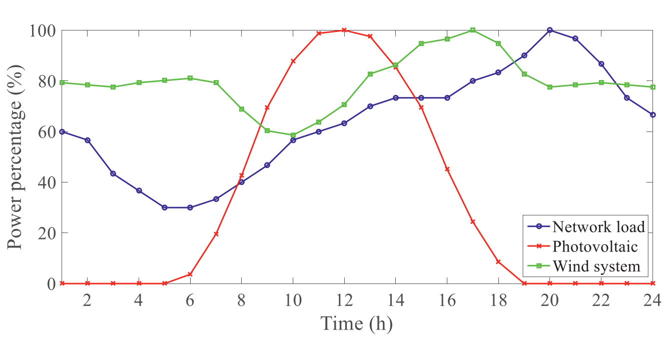

Fig. 5. Daily power percentage curves of the network load and the RESs [44].

4. Numerical analysis

4.1. Input data

The proposed model is tested on a 33-bus radial test distribution network of Fig. 4 [40] with a base power of 1 MVA and a base voltage of 12.66 kV. It is considered that the voltage should be between 0.9 and

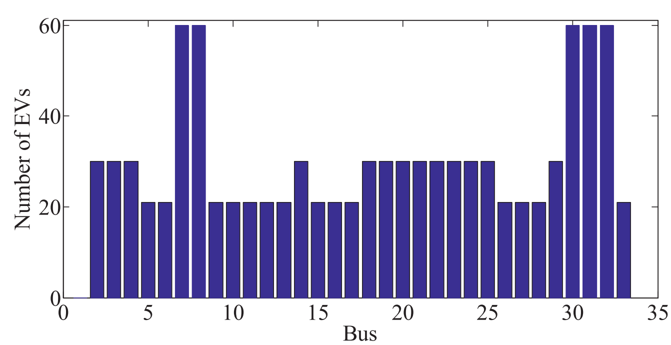

Fig. 6. Number of EVs in each bus of the network [46].

Table 2
Minima and maxima of the objective functions.

	f_1 (EC) [$]		f_2 (VDF) [p.u.]		f_3 (-SF)	
	Min	Max	Min	Max	Min	Max
f_1	1228.778	–	–	–	–	–
f_2	–	1338.379	0.407	–	–	−6.954
f_3	–	–	–	4.255	−32.672	–

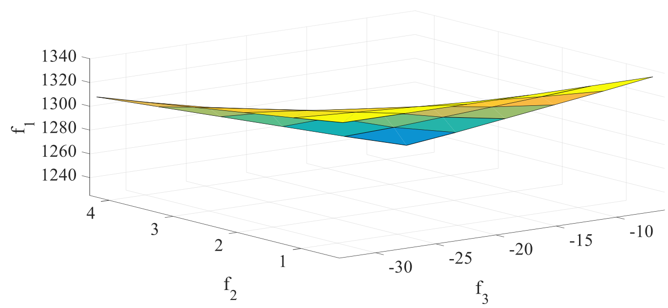

Fig. 7. Pareto front for the proposed flexible power management.

Table 3
Value of EC, VDF and SF in the best compromise solution results.

Objective function	Deterministic model	Stochastic model
f_1 (EC) [$]	1127.843	1243.127
f_2 (VDF) [p.u.]	1.0693	1.0766
f_3 (-SF)	–	−28.967

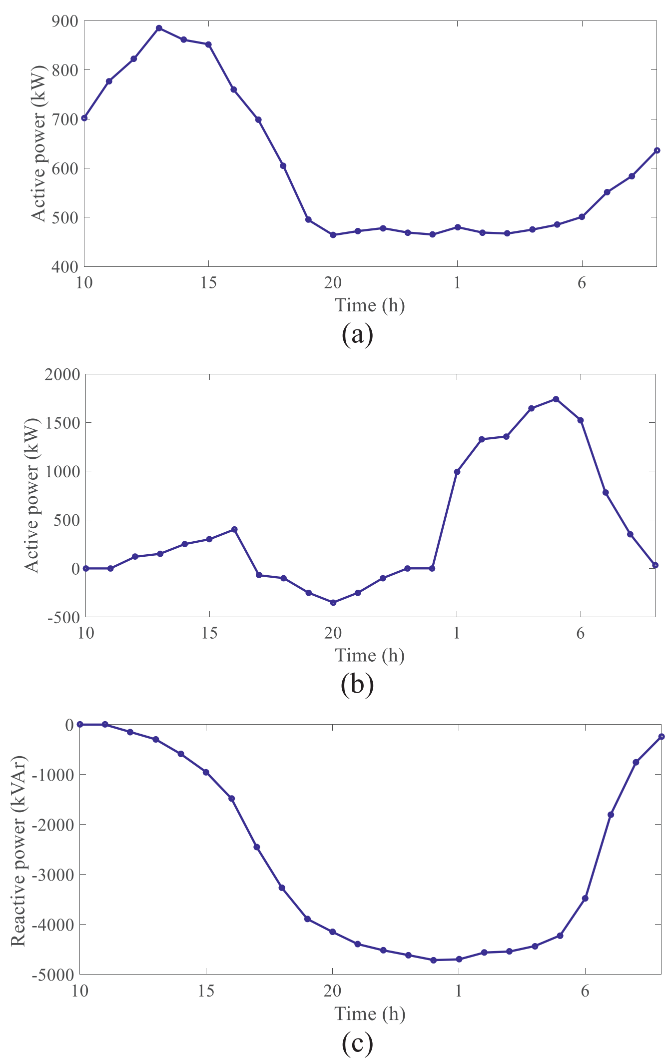

Fig. 8. Expected daily power of the RESs and the EVs;
a) active power of the RESs, b) active power of the EVs, and c) reactive power of the EVs.

1.05 p.u. [41–43], and the value of the minimum power factor in the main substation of the distribution network is equal to 0.90. The distribution lines and load data at the peak load hour are presented in [40], and the load value at other simulation times is equal to the product of the peak load and the load factor (power percentage) curve as shown in Fig. 5 based on the data of the city of Rafsanjan in Iran [44]. Further, this network includes 300 kW of WTs and 200 kW of PVs, as shown in Fig. 4. The daily power percentage curves of these RESs are shown in Fig. 5 based on the data of the city of Rafsanjan in Iran [44]. The energy prices for the periods of 1:00–7:00, 8:00–16:00 and 23:00–24:00, and 17:00–22:00 are 16, 24, and 30 $/MWh, respectively, according to [45], and k_Q is selected to be 0.08. In addition, it is considered that each of the buses 2–33 includes an EVPL, where the numbers of EVs for different buses are according to [46] as shown in Fig. 6. The charger power loss factors, i.e., a_p, a_q, b_p, and b_q, are 0.09, 0.0475, 0.02, and 0.02 [46], and other data related to EVs, such as *AER*, *SOC*, *BC*, *L*, charger/discharge rate, and charger capacity are given in [46]. Moreover, the starting time of the simulation is 10:00, and the MCS generates 1000 scenarios for uncertain parameters of the proposed problem. Thus, the backward/forward scenario reduction method yields 20 scenarios that have a high occurrence probability among these generated scenario samples.

4.2. Simulation results

The optimization model of this paper is simulated in the environment of the GAMS software and solved using the CPLEX solver [47]. Here, 5 and 45 linearization segments are selected for the voltage and circular form constraints (i.e., Eqs. (9), (10), and (18)), respectively. It is noted that the calculation error for the power/voltage variable is reported to be about 2.5%/0.5% in [32,33] for the proposed linearization method.

4.2.1. Pareto front computation

The first step in determining the Pareto front is the calculation of the minimum and maximum values of different objective functions in Eq. (1). Table 2 presents these values, where the minimum value of energy cost (EC), voltage deviation (VDF), and SF (-SF) are $1228.778, 0.407 p.u., and − 32.672, respectively, obtained by individual minimization of f_1, f_2, and f_3. The maximum values of these functions are $1338.379, 4.255 p.u., and − 6.954, which are calculated by individual minimization of f_2, f_3, and f_2, respectively. Therefore, the Pareto front for the proposed problem, Eqs. (31)–(34), is shown in Fig. 7, which is obtained according to the ε-constraint method or Algorithm 1. Accordingly, the energy cost and f_3 (-SF) will increase when VDF decreases, because, based on Table 2, the changing direction of these two functions is not the same. Finally, the optimal point of the objective functions in the best compromise solution is as given in Table 3 according to the proposed fuzzy decision-making method. It can be seen that the difference of f_1 from its minimum value is 1.15% ((1243.127–1228.778)/1243.127), and this value for f_2 and f_3 is equal to 62.2% and 12.8%, respectively. Therefore, it can be said that the energy cost is close to its minimum value with respect to the SF and VDF for the proposed problem. In addition, in Table 3 the values of the mentioned objective functions are expressed for both deterministic and stochastic modeling of uncertainties. According to Table 3, uncertainty modeling has resulted in higher energy cost and VDF than the deterministic model. This is because the stochastic modeling takes into account the conditions in which the energy consumption of loads and EVs (energy generated by RES) is more (less) than the scenario corresponding to the deterministic

Table 4
Values of the objective functions in Cases I–III.

Objective function	Case I	Case II	Case III
f_1 (EC) [$]	1391.551	1261.673	1243.127
f_2 (VDF) [p.u.]	1.1940	1.257	1.0766
f_3 (-SF)	–	–	−28.967

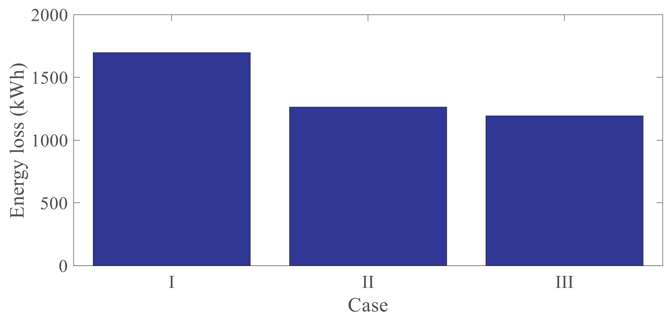

Fig. 9. Expected value of energy loss in different cases.

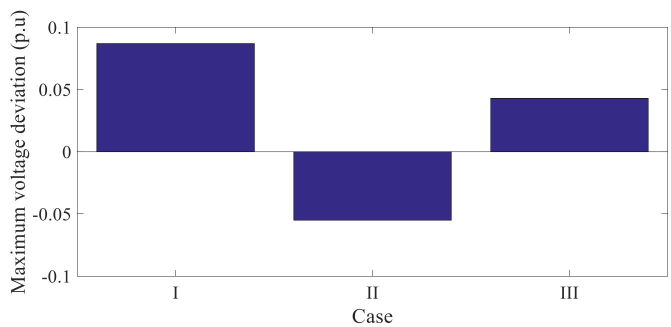

Fig. 10. Expected value of maximum voltage deviation in Cases I–III.

model. Therefore, the values of the mentioned functions in the stochastic model are more than the deterministic model. To calculate SF based on Eqs. (22)–(23), it is necessary to consider several scenarios. Therefore, it does not have a value in the deterministic model.

4.2.2. Optimal scheduling of the RESs and EVPLs

Fig. 8 shows the optimal scheduling curve of the total of RESs and EVs in the best compromise solution. According to Fig. 8(a), the RESs, i. e., PV and WT, inject more active power into the network at hours 10:00–17:00 compared with the other hours. Hence, in this period, the EVs will absorb the active power from RESs or local sources and inject the low reactive power into the network based on Fig. 8(b) and (c) because of voltage regulation. However, in the period of 18:00–22:00, which is related to the peak-load times based on Fig. 5, the EVs and the RESs inject a low active power and the EVs inject a high reactive power into the distribution network to regulate voltage, reduce energy cost, and obtain a high SF. In addition, the EVs receive a high active power from the RESs and the distribution network in the period from 1:00 to 7:00 to provide their energy consumption in the trips because of the low energy price in these hours based on Section 4.1. Hence, they will inject a high amount of reactive power into the network for regulating the voltage profile. Finally, it is pointed out that the daily scheduling power curve of EVs is set to achieve the least energy cost, make the voltage profile as flat as possible, and increase the SF as shown in Fig. 8.

4.2.3. Capabilities of the proposed flexible power management

To analyze the capabilities of the proposed strategy, three cases are implemented in this section as follows:

-

Case IPower flow analysis in the distribution network without considering the RESs and the EVPLs;

-

Case IIPower flow analysis in the distribution network considering the RESs;

-

Case IIIMultiobjective flexible power management in the distribution network considering the RESs and the EVPLs (based on model (31)–(34)).

The results of this section are given in Table 4 and Figs. 9 and 10, which present the values of the objective functions, daily energy loss, and maximum voltage deviation, respectively, in the different cases. Owing to the presence of RESs in the distribution network, Case II, the energy cost and energy loss are reduced in comparison with Case I because of the local energy supply to customers by RESs. However, the value of the VDF and the maximum voltage deviation increase in this case compared with Case I as a result of the high injection of active power by RESs. Therefore, an overvoltage occurs in this case as shown in Fig. 10. Nevertheless, it is noted that with the proposed flexible power management in the smart distribution network using EVPLs, as in Case III, the least energy cost, minimum energy loss, minimum VDF, and the highest flexibility can be obtained, as reported in Table 4 and Figs. 9 and 10, compared with Cases I and II. Thus, the energy cost is reduced about to 10.67% ((1391.551–1243.127)/1391.551)/1.47% ((1261.673–1243.127)/1261.673) compared with Case I/II. Furthermore, in Case III, the VDF can be decreased by about 9.83% ((1.1940–1.0766)/1.1940)/14.35% ((1.257–1.0766)/1.257) in comparison with Case I/II. This value for energy loss in Case III is 27.7%/8.33% in comparison with Case I/II. Moreover, Case III can yield a system flexibility of 28.967 for the distribution network, whereas this index is not considered in Cases I and II. Thus, defining the proposed flexible power management strategy for a smart distribution network including controllable loads, such as EVPLs, can improve the technical and economic indices while they are not optimal and suitable in Cases I and II. Moreover, the flexibility of the distribution network will be increased with flexible sources, such as EVPLs. In other words, the main capability of ECPLs is to improve the network flexibility in the presence of RESs.

5. Conclusions

In this paper, multiobjective flexible power management in an SDN including RESs and EVPLs was presented. The NLP model of this problem minimizes the energy cost and voltage deviation functions and maximizes the system flexibility subject to the AC load flow equations in the presence of RESs, WTs, PVs, and EVPLs. In the next step to achieve the globally optimal solution and speed up the calculation, the equivalent linear formulation is adopted. The multiobjective model of this formulation is based on the hybrid ε-constraint and fuzzy decision-making methods. This problem also includes uncertainties of the load, energy price, RES power, EV energy demand, and power production capacity. Therefore, stochastic programming according to the Monte Carlo simulation and the fast backward/forward scenario reduction was used to model these uncertain parameters. According to the numerical results, the proposed flexible power management can reduce energy cost, energy loss, and voltage deviation, and it will yield a flat voltage profile and a high system flexibility by using the optimal operation of EV parking lots. Also at the compromise point, the mentioned objective functions are a small distance from their minimum value, so that the energy cost, voltage deviation function, and system flexibility are about 1%, 62%, and 13% of their minimum value, respectively. The proposed scheme with EV energy management has been able to improve energy costs, energy losses, and voltage profiles compared to the network flow distribution by about 11%, 28%, and 10%, respectively. Under these conditions, it increases the flexibility of the system up to 30. It should be said that these results and capabilities can be achieved in real networks by implementing the proposed strategy to this power system.

Note that in function $f1$ in Eq. (1), only the cost of purchasing energy (charging) of EVs is considered. Therefore, the optimal operation of SDN is done based on this case. In $f1$, when the EVs are in charging mode, the power flowing through the distribution substation (P^G) will be higher than in the case without the EVs, so the extra cost represents the cost of charging the EVs. In addition, energy sales revenue by EVs in discharge mode is also calculated in the function. Thus, the mentioned function considers the net cost of EVs for their charge. However, the cost of deregulation and the cost of their capacity were not considered. Capacity cost is not taken into account because it is assumed that the size of the parking lots is known, an operation problem is given for it. If a planning problem is presented, capacity cost can be considered. Therefore, this was suggested as a future work.

CRedit authorship contribution statement

Afshin Pirouzi: Conceptualization, Methodology, Software, Writing- Original draft preparation.
Jamshid Aghaei: Supervision, Conceptualization, Methodology, Writing- Reviewing and Editing.
Sasan Pirouzi: Writing- Original draft preparation, Methodology, Data curation, Visualization, Investigation.
Vahid Vahidinasab: Supervision, Writing- Reviewing and Editing.
Ahmad Rezaee Jordehi: Writing- Original draft preparation, Software, Visualization, Investigation.

Declaration of competing interest

The authors declare that they have no known competing financial interests or personal relationships that could have appeared to influence the work reported in this paper.

Acknowledgment

The authors thank Dr. Hanna Niemelä for her assistance with proofreading of the paper and comments that greatly improved the manuscript.

References

[1] Eurelectric, Flexibility and Aggregation Requirements for Their Interaction in the Market, Eurelectric, 2014.
[2] J. Aghaei, M. Barani, M. Shafie-khah, J.P.S. Catalão, A.A.S.d.l. Nieta, Risk-constrained offering strategy for aggregated hybrid power plant including wind power producer and demand response provider, IEEE Transactions on Sustainable Energy 7 (2) (2016) 513–525.
[3] N. Helisto, J. Kiviluoma, H. Holttinen, Long-term impact of variable generation and demand side flexibility on thermal power generation, IET Renew. Power Gener. 12 (6) (2018) 718–726.
[4] Y. Zhang, Z.Y. Dong, F. Luo, Y. Zheng, K. Meng, K.P. Wong, Optimal allocation of battery energy storage systems in distribution networks with high wind power penetration, IET Renew. Power Gener. 10 (8) (2016) 1105–1113.
[5] M.C. Kisacikoglu, Vehicle-to-Grid Reactive Power Operation Analysis of the EV/PHEV Bidirectional Battery Charger, Tennessee University, 2013.
[6] Z. Liu, Q. Wu, S. Huang, L. Wang, M. Shahidehpour, Y. Xue, Optimal day-ahead charging scheduling of electric vehicles through an aggregative game model, IEEE Trans. Smart Grid 9 (5) (2018) 5173–5184.
[7] R.F. Atallah, C.M. Assi, W. Fawaz, M.H.K. Tushar, M.J. Khabbaz, Optimal supercharge scheduling of electric vehicles: centralized versus decentralized methods, IEEE Trans. Veh. Technol. 67 (9) (2018) 7896–7909.
[8] Z. Liu, Q. Wu, K. Ma, M. Shahidehpour, Y. Xue, S. Huang, Two-stage optimal scheduling of electric vehicle charging based on transactive control, IEEE Trans. Smart Grid 10 (3) (2019) 2948–2958.
[9] Y. Zheng, Y. Song, D.J. Hill, K. Meng, Online distributed MPC-based optimal scheduling for EV charging stations in distribution systems, IEEE Trans. Ind. Informatics 15 (2) (2019) 638–649.
[10] X. Zhu, H. Han, S. Gao, Q. Shi, H. Cui, G. Zu, A multi-stage optimization approach for active distribution network scheduling considering coordinated electrical vehicle charging strategy, IEEE Access 6 (2018) 50117–50130.
[11] Y. Li, K. Li, Incorporating demand response of electric vehicles in scheduling of isolated microgrids with renewables using a bi-level programming approach, IEEE Access 7 (2019) 116256–116266.
[12] Y. Zhou, D.K.Y. Yau, P. You, P. Cheng, Optimal-cost scheduling of electrical vehicle charging under uncertainty, IEEE Trans. Smart Grid 9 (5) (2018) 4547–4554.
[13] M. Latifi, A. Rastegarnia, A. Khalili, S. Sanei, Agent-based decentralized optimal charging strategy for plug-in electric vehicles, IEEE Trans. Ind. Electron. 66 (5) (2019) 3668–3680.
[14] H. Chung, W. Li, C. Yuen, C. Wen, N. Crespi, Electric vehicle charge scheduling mechanism to maximize cost efficiency and user convenience, IEEE Trans. Smart Grid 10 (3) (2019) 3020–3030.
[15] J. Chen, et al., Electric vehicle charging schedule considering user's charging selection from economics, IET Gener. Transm. Distrib. 13 (15) (2019) 3388–3396, 6 8.
[16] M. Maigha, M.L. Crow, Electric vehicle scheduling considering co-optimized customer and system objectives, IEEE Trans. Sustain. Energy 9 (1) (2018) 410–419.
[17] W. Jiang, Y. Zhen, A real-time EV charging scheduling for parking lots with PV system and energy store system, IEEE Access 7 (2019) 86184–86193.
[18] F. Ahmad, A. Iqbal, I. Ashraf, M. Marzband, I. Khan, Optimal location of electric vehicle charging station and its impact on distribution network: a review, Energy Reports 8 (2022) 2314–2333.
[19] D. Sadeghi, N. Amiri, M. Marzband, A. Abusorrah, K. Sedraoui, Optimal sizing of hybrid renewable energy systems by considering power sharing and electric vehicles, Int. J. Energy Res. 46 (6) (2022) 8288–8312.
[20] M.A. Baherifard, R. Kazemzadeh, A. Sadeghi Yazdankhah, M. Marzband, Intelligent charging planning for electric vehicle commercial parking lots and its impact on distribution network's imbalance indices, Sustain. Energy Grids Netw. 30 (2022), 100620.
[21] S.E. Ahmadi, D. Sadeghi, M. Marzband, A. Abusorrah, K. Sedraoui, Decentralized bi-level stochastic optimization approach for multi-agent multi-energy networked micro-grids with multi-energy storage technologies, Energy 245 (2022), 123223.
[22] S.M. Kazemi-Razi, H. Askarian Abyaneh, H. Nafisi, Z. Ali, M. Marzband, Enhancement of flexibility in multi-energy microgrids considering voltage and congestion improvement: robust thermal comfort against reserve calls, Sustain. Cities Soc. 74 (2021), 103160.
[23] N. Nasiri, S. Zeynali, S. Najafi Ravadanegh, M. Marzband, A hybrid robust-stochastic approach for strategic scheduling of a multi-energy system as a price-maker player in day-ahead wholesale market, Energy 235 (2021), 121398.
[24] P. Akbary, et al., Extracting appropriate nodal marginal prices for all types of committed reserve, Comput. Econ. 53 (2019) 1–26.
[25] Z. Yang, et al., Robust multi-objective optimal design of islanded hybrid system with renewable and diesel sources/stationary and mobile energy storage systems, Renew. Sust. Energ. Rev. 148 (2021), 111295.
[26] J. Liu, et al., An IGDT-based risk-involved optimal bidding strategy for hydrogen storage-based intelligent parking lot of electric vehicles, J. Energy Storage 27 (2020), 101057.
[27] M. Mir, et al., Application of hybrid forecast engine based intelligent algorithm and feature selection for wind signal prediction, Evol. Syst. 11 (2020) 559–573.
[28] M. Mehrpooya, N. Ghadimi, M. Marefati, S.A. Ghorbanian, Numerical investigation of a new combined energy system includes parabolic dish solar collector, stirling engine and thermoelectric device, Int. J. Energy Res. 45 (11) (2021) 16436–16455.
[29] F. Mirzapour, et al., A new prediction model of battery and wind-solar output in hybrid power system, J. Ambient Intell. Hum. Comput. 10 (2019) 77–87.
[30] W. Cai, et al., Optimal bidding and offering strategies of compressed air energy storage: a hybrid robust-stochastic approach, Renew. Energy 143 (2019) 1–8.
[31] S. Pirouzi, et al., Power conditioning of distribution networks via single-phase electric vehicles equipped, IEEE Syst. J. 13 (3) (Sept. 2019) 3433–3442.
[32] J. Aghaei, S.A. Bozorgavari, S. Pirouzi, H. Farahmand, M. Korpås, Flexibility planning of distributed battery energy storage systems in smart distribution networks, Iran. J. Sci. Technol. Trans. Electr. Eng. (2019) 1–17, vol. PP.
[33] S.A.F. Asl, et al., A new two-layer model for energy management in the smart distribution network containing flexi-renewable virtual power plant, Electr. Power Syst. Res. 194 (2021), 107085.
[34] H. Kiani, et al., Adaptive robust operation of the active distribution network including renewable and flexible sources, Sustain. Energy Grids Netw. 26 (2021), 100476.
[35] A. Dini, et al., IA flexible-reliable operation optimization model of the networked energy hubs with distributed generations, energy storage systems and demand response, Energy 239 (2022), 121923.
[36] M.R. Ansari, S. Pirouzi, M. Kazemi, A. Naderipour, M. Benbouzid, Renewable generation and transmission expansion planning coordination with energy storage system: a flexibility point of view, Appl. Sci. 11 (8) (2021) 3303.
[37] S.M. Mohseni-Bonab, A. Rabiee, Be. Mohammadi-Ivatloo, Voltage stability constrained multi-objective optimal reactive power dispatch under load and wind power uncertainties: a stochastic approach, Renew. Energy 85 (2016) 598–609.
[38] B. Khorramdel, H. Khorramdel, J. Aghaei, A. Heidari, V.G. Agelidis, Voltage security considerations in optimal operation of BEVs/PHEVs integrated microgrids, IEEE Trans. Smart Grid 6 (4) (2015) 1575–1587.
[39] A. Kavousi-Fard, A. Khodaei, Efficient integration of plug-in electric vehicles via reconfigurable microgrids, Energy 111 (2016) 653–663.
[40] P.R. Babu, C.P. Rakesh, G. Srikanth, M.N. Kumar, D.P. Reddy, A novel approach for solving distribution networks, in: India Conference (INDICON), 2009Annual IEEE, 2009, pp. 1–5.
[41] A. Dini, A.R. Azarhooshang, S. Pirouzi, M.A. Norouzi, M. Lehtonen, Security-constrained generation and transmission expansion planning based on optimal

bidding in the energy and reserve markets, Electr. Power Syst. Res. 193 (2021), 107017.
[42] M.A. Norouzi, et al., Hybrid stochastic/robust flexible and reliable scheduling of secure networked microgrids with electric springs and electric vehicles, Appl. Energy 300 (2021), 117395.
[43] M.A. Norouzi, J. Aghaei, S. Pirouzi, Enhancing distribution network indices using electric spring under renewable generation permission, in: International Conference on Smart Energy Systems and Technologies (SEST), 2019, pp. 1–6.
[44] A. Maleki, A. Askarzadeh, Optimal sizing of a PV/wind/diesel system with battery storage for electrification to an off-grid remote region: a case study of Rafsanjan, Iran, Sustain. Energy Technol. Assess. 7 (2014) 147–153.
[45] S. Shafiee, M. Fotuhi-Firuzabad, M. Rastegar, Impacts of controlled and uncontrolled PHEV charging on distribution systems, in: 9th IET Int. Conf. Advances in Power System Control, Operation and Management (APSCOM 2012), 2013, pp. 1–6.
[46] S. Pirouzi, M.A. Latify, G.R. Yousefi, Investigation on reactive power support capability of PEVs in distribution network operation, in: 23rd Iranian Conference on Electrical Engineering (ICEE), 2015.
[47] Generalized Algebraic Modeling Systems (GAMS). [Online]. Available: http://www.gams.com.